TRANSITIONS AND INSTABILITIES OF FLOW IN A SYMMETRIC CHANNEL WITH A SUDDENLY EXPANDED AND CONTRACTED PART

Jiro Mizushima, Takahiro Adachi and Yukinobu Shiotani
Department of Mechanical Engineering
Doshisha University
Tatara Miyakodani 1-3, Kyotanabe, Kyoto 610-0321, Japan

ABSTRACT

Transitions and instabilities of flow in a symmetric channel with a suddenly expanded and contracted part are investigated numerically by three different methods, i.e. the time marching method for dynamical equations, the SOR iterative method and finite element method for steady state equations. Numerical results are analyzed by using the bifurcation theory. Linear and weakly nonlinear stability theories are also applied to the flow. It is known that the flow is steady and symmetric at low Reynolds numbers, becomes asymmetric at a critical Reynolds number, gets symmetric again at another critical Reynolds number and becomes oscillatory. Multiple stable steady solutions are found in some cases and the parameter range of existence of the multiple stable solutions is obtained. Impinging free shear layer instabilities are found to cause the flow oscillations, and the mechanism of this instability is clarified.

INTRODUCTION

Two-dimensional flow with a suddenly expanded and contracted part is a typical example which is not homogeneous in its flow direction. Traditional stability theories for parallel flows can not be applied to such a flow because of the inhomogeneity. So, the stability of the flow has been investigated mainly by numerical methods. It has been revealed that the transitions and instabilities of the flow include rich physics.

Symmetric sudden expansion flow has been investigated extensively. For instance, Durst, Melling and Whitelaw (1974) and Cherdron, Durst and Whitelaw (1978) measured velocity profiles in detail for the symmetric sudden expansion flow by L.D.V. and flow visualization methods. It is found that the flow is symmetric at low Reynolds numbers, but becomes asymmetric at higher Reynolds numbers. The origin of the steady asymmetric flows in a symmetric sudden expansion was clarified by Fearn, Mullin and Cliffe (1990) by using experimental and numerical techniques. They showed that the asymmetry arises at a critical Reynolds number due to a pitchfork bifurcation and evaluated the critical Reynolds number. It was also shown that this pitchfork bifurcation becomes inevitably imperfect due to a minimal asymmetry of the flow channel. They observed time-dependent flows at higher Reynolds numbers and attributed the appearance of the unsteadiness to three-dimensional effects. Alleborn, Nandakumar, Raszillier and Durst (1997) investigated the flow pattern in the same channel by numerical simulations, and obtained a bifurcation diagram of the equilibrium solutions. They investigated the instability of the equilibrium solutions by the linear stability theory.

The transitions and bifurcations of flow in a two-dimensional symmetric channel with a suddenly expanded and contracted part was investigated by Mizushima, Yamaguchi and Okamoto (1996), which we call MYO in short hereafter. They made numerical simulations for the flow and analyzed the numerical data by the bifurcation theory. It was found that the flow is steady and symmetric at low Reynolds numbers, becomes asymmetric at a critical Reynolds number Re_{c1} due to a symmetry breaking pitchfork bifurcation and gets symmetric again at $Re_{c2}(> Re_{c1})$ due to another pitchfork bifurcation. The symmetric flow was shown to become oscillatory in time at Re_{c3} due to a Hopf bifurcation. They evaluated the critical values of Re_{c1}, Re_{c2} and Re_{c3}, and obtained a transition diagram of the flow. However, the bifurcation diagrams obtained were incomplete because the diagrams included unexpected discontinuous lines in place of presumably smooth lines.

Transitions and instabilities of flow in a symmetric

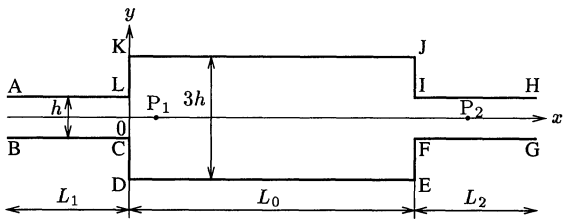

Figure 1. Channel geometry and coordinates.

channel with a suddenly expanded and contracted part are investigated numerically by three different methods, i.e. the time marching method for dynamical equations, the SOR iterative method and the finite element method for steady state equations in this paper. This work is an extension of MYO. We focus our attention to the multiple stable steady solutions of the flow at relatively low Reynolds numbers and the impinging free shear layer instability when the flow becomes periodic in time. Linear and weakly nonlinear stability theories are also applied to the flow and coefficients of an amplitude equation are evaluated numerically for the symmetry breaking pitchfork bifurcation at Re_{c1}.

FORMULATION AND NUMERICAL METHODS

Formulation

We consider a flow in a symmetric channel with a suddenly expanded and contracted part (Fig. 1). Flow enters from the inlet AB of width h into the suddenly expanded part DEJK through the sudden expansion LC, leaves it through the sudden contraction IF and goes out from the outlet HG of width h. The expansion ratio $E \equiv$ DK/LC is fixed as $E = 3$ in the present study. The aspect ratio A is defined as $A = L/3h =$ DE/KD where L is the length of the suddenly expanded part.

The flow is assumed two-dimensional and incompressible. The governing equations for the velocity $\mathbf{u} = (u, v)$ and the pressure p, i. e. the Navier-Stokes equation and the continuity equation, are written in a nondimensional form as

$$\frac{\partial \mathbf{u}}{\partial t} + (\mathbf{u} \cdot \nabla)\mathbf{u} = -\nabla p + \frac{1}{Re}\nabla^2 \mathbf{u}, \tag{1}$$

$$\nabla \cdot \mathbf{u} = 0, \tag{2}$$

where all the variables are normalized by the maximum inlet velocity $U_{\max}$ and the half channel width $h/2$ of the inlet channel. The Reynolds number is defined as $Re = U_{\max} h/2\nu$. As the flow is assumed two-dimensional, the stream function $\psi(x, y, t)$ can be introduced. So, we use the vorticity $\omega(x, y, t)$ and the stream function $\psi(x, y, t)$ in our formulation. The vorticity transport and poisson equations are written as

$$\frac{\partial \omega}{\partial t} + \frac{\partial \psi}{\partial y}\frac{\partial \omega}{\partial x} - \frac{\partial \psi}{\partial x}\frac{\partial \omega}{\partial y} = \frac{1}{Re}\left(\frac{\partial^2 \omega}{\partial x^2} + \frac{\partial^2 \omega}{\partial y^2}\right), \tag{3}$$

$$\omega = -\left(\frac{\partial^2 \psi}{\partial x^2} + \frac{\partial^2 \psi}{\partial y^2}\right). \tag{4}$$

The boundary condition at AB is assumed as a fully developed plane Poiseuille flow so that,

$$\frac{\partial \psi}{\partial x} = 0, \quad \frac{\partial \omega}{\partial x} = 0,$$

$$\psi = \int_{-1}^{y} u dy = \int_{-1}^{y} (1 - y^2) dy = y(1 - \frac{y^2}{3}) + \frac{2}{3}. \tag{5}$$

The outlet condition at HG is given as

$$\frac{\partial^2 \psi}{\partial x^2} = 0, \quad \frac{\partial^2 \omega}{\partial x^2} = 0, \tag{6}$$

when the resultant flow is steady. On the other hand, in the case where the flow becomes periodic in time, the Sommerfeld radiation condition is adopted at the outlet, which is expressed as,

$$\frac{\partial \psi}{\partial t} + c\frac{\partial \psi}{\partial x} = 0, \quad \frac{\partial \omega}{\partial t} + c\frac{\partial \omega}{\partial x} = 0, \tag{7}$$

where c is a phase velocity and the velocity of u at each position on HG is simply used for the value of c in the present study.

The boundary conditions on all the walls are non-slip condition, so the values of the stream function on the walls are determined as

$$\psi = \psi_1 = 0 \quad \text{on BCDEFG},$$

$$\psi = \psi_2 = 4/3 \quad \text{on HIJKLA},$$

$$\frac{\partial \psi}{\partial x} = 0, \quad \frac{\partial \psi}{\partial y} = 0 \quad \text{on BCDEFG and HIJKLA}, \tag{8}$$

because the volumetric flow rate in each cross section of the channel is constant.

Time marching method

In the time marching method, an equally spaced mesh system with $\Delta x = \Delta y = 0.1$ is used. The vorticity transport equation (3) is solved by the explicit Euler method with the first order accuracy in time together with the 2nd order accuracy of central finite difference in space. The time increment Δt is chosen as $\Delta t = 0.001$ or $\Delta t = 0.0005$. The Poisson equation (4) is descretized by the 2nd order central finite difference and solved by the SOR method, where the relaxation factor ϵ is kept as $\epsilon = 1.5$. The convergence of the SOR method is determined when the maximum relative error reaches 10^{-5} and the steady flow state is determined when the stream function becomes time independent and the maximum relative error reaches 10^{-10}.

SOR iterative method

Both the steady state vorticity transport equation obtained by putting $\partial/\partial t = 0$ in eq. (3) and the Poisson equation (4) are solved by the SOR iterative method. Spatial derivatives are approximated by the fourth order finite differences. The relaxation factor ϵ for the SOR method is determined in the range $0.7 < \epsilon < 1.0$ by considering aspect ratios and Reynolds numbers.

The convergence of the SOR method is determined when the maximum relative error reaches 10^{-10}. In order to calculate unstable steady symmetric solutions, the SOR method is utilized under the symmetry condition along the center line of the channel.

Finite element method

The computational domain is divided by triangular elements in the finite element method. Primitive variables (u, v) and p are used for the numerical calculations. The velocities u and v are approximated by quadratic-polynomial expressions using six nodes in each element and the pressure is approximated by linear-function expressions using three nodes. These expressions for u, v and p are substituted in the steady state Navie-Stokes equation (1) after putting $\partial/\partial t = 0$, and the continuity equation (2). The descretized equations are obtained by using Galerkin's method and are solved numerically by using the Newton-Raphson method. The node number used is 4163 and the element number is 1992. The convergence of the Newton-Raphson method is determined when the maximum relative error reaches 10^{-10}.

Linear stability of steady state solutions

For the linear stability analysis, we express the steady state solution by $\omega = \bar{\omega}(x, y)$ and $\psi = \bar{\psi}(x, y)$ and add a disturbance $\omega'(x, y, t)$ and $\psi'(x, y, t)$ to them. Then the vorticity and the stream function are written as $\omega = \bar{\omega} + \bar{\omega}'$ and $\psi = \bar{\psi} + \psi'$. By substituting the expressions for ω and ψ into eqs. (3) and (4), neglecting the nonlinear terms of the disturbances and assuming the time dependence of the disturbance as $\omega' = \hat{\omega}(x, y)\exp(\lambda t)$ and $\psi' = \hat{\psi}(x, y)\exp(\lambda t)$, we obtain the linear stability equations as

$$\lambda\hat{\omega} = -\frac{\partial\bar{\psi}}{\partial y}\frac{\partial\hat{\omega}}{\partial x} - \frac{\partial\hat{\psi}}{\partial y}\frac{\partial\bar{\omega}}{\partial x} + \frac{\partial\bar{\psi}}{\partial x}\frac{\partial\hat{\omega}}{\partial y} + \frac{\partial\hat{\psi}}{\partial x}\frac{\partial\bar{\omega}}{\partial y} + \frac{1}{Re}\left(\frac{\partial^2\hat{\omega}}{\partial x^2} + \frac{\partial^2\hat{\omega}}{\partial y^2}\right), \tag{9}$$

$$\hat{\omega} = -\left(\frac{\partial^2\hat{\psi}}{\partial x^2} + \frac{\partial^2\hat{\psi}}{\partial y^2}\right), \tag{10}$$

where λ is the linear growth rate of the disturbance. The equations (10) and (11) are solved by the SOR iterative method and the value λ is evaluated. The steady state solution is judged as stable or unstable according to the sign of the real part of λ.

Weakly nonlinear stability

The nonlinear behavior of the solution near the critical state of the symmetry breaking pitchfork bifurcation is analyzed by the weakly nonlinear stability theory.

The standard procedure of the weakly nonlinear stability theory leads to an amplitude equation for $A(t)$ as,

$$\frac{dA}{dt} = \lambda_0 A + \lambda_1 A^3, \tag{11}$$

where $A(t)$ is the amplitude of the disturbance and is identified as the magnitude of v at $P_1 = (0.4h, 0)$ in Fig. 1.

It is noted here that a relation $\lambda = \lambda_0(1/Re_c - 1/Re)$ holds near the critical state of the pitchfork bifurcation.

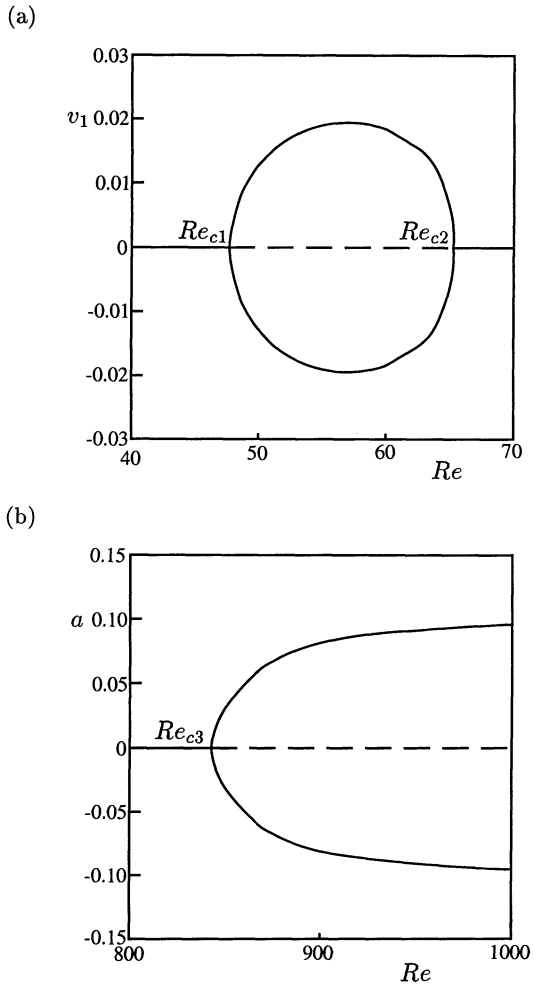

Figure 2. Bifurcation diagram. $A = 7/3$. (a) Velocity v_1 at $(x, y) = (0.8, 0.0)$. (b) Amplitude of oscillation a.

NUMERICAL METHODS

Transitions of the flow

Case of $A = 7/3$. The transitions of flow for the case of $A = 7/3$ were investigated by Mizushima, Yamaguchi and Okamoto (MYO), so their results are reviewed briefly. The bifurcation diagrams for $A = 7/3$ are reproduced in Figs. 2(a) and 2(b), where the velocity v_1 in the y-direction at $P_1(x, y) = (0.4h, 0)$ is taken as a representative value manifesting the magnitude of the asymmetry and the amplitude a of the velocity v at $(x, y) = (8.5h, 0)$ respectively. The solid and dashed

lines indicate the stable and unstable solutions in these figures.

For the Reynolds numbers Re smaller than $Re_{c1}(=47.7)$, there is only one stable steady solution with $v_1 = 0$, i. e. the flow is symmetric as seen in Fig. 2(a). At Re_{c1} the line of v_1 branches into three, which shows that there appear two stable asymmetric solutions while the symmetric solution becomes unstable. The two stable and one unstable solutions join into one stable solution at $Re_{c2}(= 65.2)$, which shows another pitchfork bifurcation.

The steady state solution is unique for $Re_{c2} < Re < Re_{c3}$ as seen from Fig. 2(b), which is a stable symmetric flow. The symmetric flow becomes unstable, and an oscillatory flow appears at $Re_{c3}(= 843)$ due to the Hopf bifurcation.

Linear stability of the symmetric steady flow has not been confirmed by MYO. We have evaluated the linear growth rate of the symmetric flow in the range of $40 \leq Re \leq 70$ by solving eqs. (9) and (10) with the SOR method. The linear growth rate λ is depicted in Fig. 3. It is needless to say that the critical Reynolds numbers Re_{c1} and Re_{c2} agree with the values obtained by the bifurcation analysis of the numerical data. It is seen that the symmetric flow is unstable in the range of $Re_{c1} < Re < Re_{c2}$ and that it is stable out of the range.

The weakly nonlinear stability theory is applied near the pitchfork bifurcation point at Re_{c1}. The coefficients of the amplitude equation (11) are evaluated by the SOR iterative method as $\lambda_0 = 1.113$ and $\lambda_1 = -6.804$. The representative velocity v_1 is calculated from eq. (11) and is shown in Fig. 4 together with the results of numerical results from the full nonlinear equations.

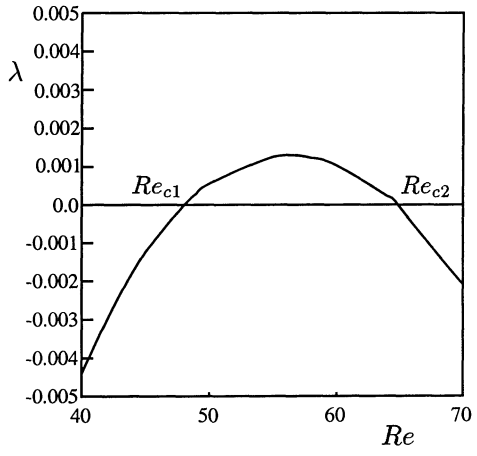

Figure 3. Linear growth rate λ. $A = 7/3$.

Case of $A = 8/3$. The transition diagrams for $A = 8/3$ obtained by MYO were incomplete because the solution lines for v_1 had discontinuities in place of pre-

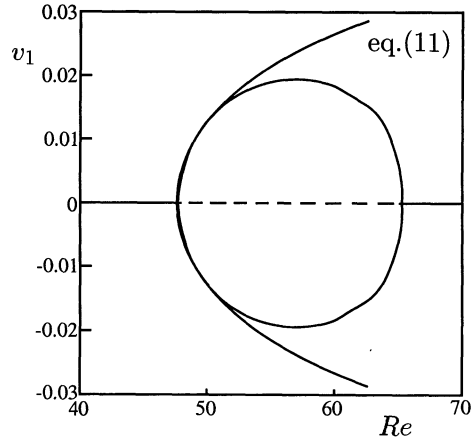

Figure 4. Bifurcation diagram obtained by the weakly nonlinear stability theory (eq. (11)).

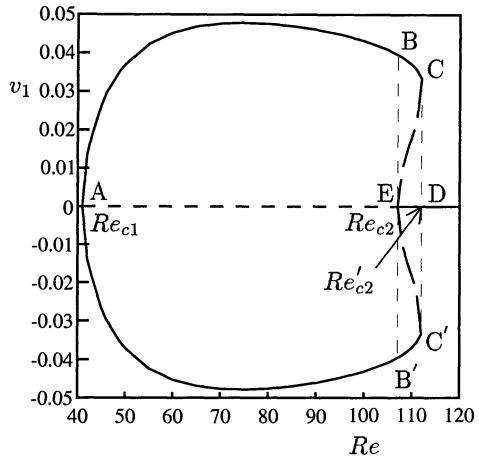

Figure 5. Bifurcation diagram. $A = 8/3$.

sumably continuous lines. MYO speculated that the discontinuities occur because of the inverse pitchfork bifurcation. We confirm their speculation by utilizing the finite element method.

We have calculated the steady solutions for $A = 8/3$ in detail. The bifurcation diagram obtained is depicted in Fig. 5. The solid and dashed lines indicate the stable and unstable steady state solutions respectively. The symmetric unstable solutions with $v_1 = 0$ were obtained by the SOR method with the finite difference approximation under the symmetry condition along the center line, whereas unstable solutions with $v_1 \neq 0$ were obtained by the finite element method.

The first symmetry breaking pitchfork bifurcation occurs at A in Fig. 5, where the symmetric solution becomes unstable. The bifurcated solutions are indicated by ABCE and AB′C′E. The asymmetric solution ABC and AB′C′ are stable, but make saddle node bifurcations at C or C′ ($Re = Re'_{c2}$) respectively. The

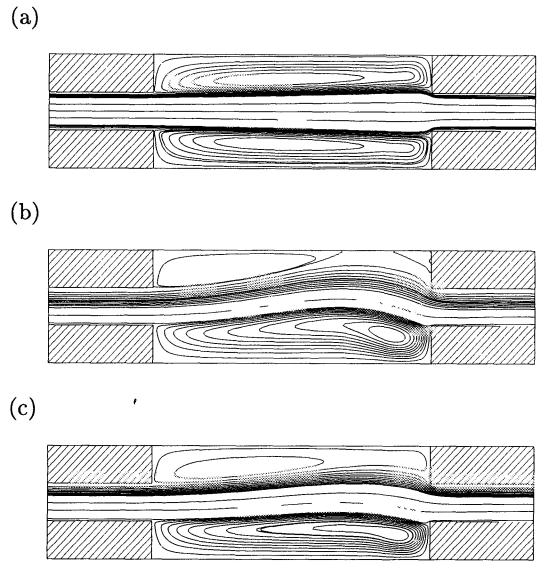

Figure 6. Flow fields. $Re = 110$.(a) Stable symmetric flow. (b) Stable asymmetric flow. (c) Unstable asymmetric flow.

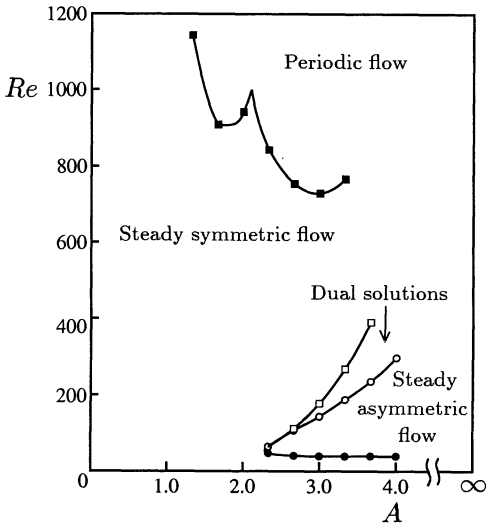

Figure 7. Transition diagram. Filled circles: first symmetry breaking pitchfork bifurcation, Re_{c1}. Open circles: second symmetry recovering pitchfork bifurcation, Re_{c2}. Open squares: saddle node bifurcation, Re'_{c2}. Filled squares: Hopf bifurcation, Re_{c3}.

asymmetric solutions CE and C'E are unstable and the symmetric solution ED is stable. So, there are three stable solutions and two unstable solutions in the range of $Re_{c2} < Re < Re'_{c2}$.

The critical values of the pitchfork and saddle node bifurcations are evaluated numerically as $Re_{c1} = 41.0$, $Re_{c2} = 107$ and $Re'_{c2} = 112$. The critical values of Re_{c1} and Re'_{c2} are in good agreement with those by MYO, while Re_{c2} had not been obtained by MYO.

We can easily imagine from Fig. 5 that there occurs a hysteresis phenomenon. If the Reynolds number is increased from a small value, the symmetric solution bifurcates at A. The bifurcated solution takes a route indicated by ABCD or ABC'D'. This shows that the asymmetric flow indicated by ABC (or ABC') make a transition from C (or C') to D at Re'_{c2}. On the other hand, if the Reynolds number is decreased from a large value, the symmetric flow become unstable at E and make a transition to B at $Re = Re_{c2}$ and take a route indicated by DEBA (or DEB'A). Thus the hysteresis phenomenon occurs in the range of $Re_{c2} \leq Re \leq Re'_{c2}$.

The flow patterns of the two stable asymmetric solutions, a stable symmetric solution and unstable asymmetric solutions at $Re = 110$, which lies between Re_{c2} and Re'_{c2}, are shown in Figs. 6(a) - (c). There are two large recirculation vortices which extend in the full length of the expanded part in the stable symmetric flow (Fig. 6(a)). The stable asymmetric flow (Fig. 6(b)) bends much more than the unstable asymmetric flow (Fig. 6(c)) as easily understood also from Fig. 5.

Transition diagram

We made numerical calculations for various aspect ratios A and obtained a transition diagram as summarized in Fig. 7. For $A < A_c (= 2.3)$, the flow does not experience any pitchfork bifurcations and makes a transition from a steady symmetric flow to an oscillatory flow at Re_{c3} (line with filled squares). For $A > A_c$, the flow undergoes a transition from a steady symmetric flow to a steady asymmetric flow at Re_{c1} (the line with filled circles) due to the symmetry breaking pitchfork bifurcation, and becomes symmetric again at Re'_{c2} (line with open squares). There are multiple stable solutions in the range of $Re_{c2} < Re < Re'_{c2}$, which is the region between lines with open circles and filled circles.

The steady flow makes a transition from the steady symmetric flow to an oscillatory flow due to the Hopf bifurcation at Re_{c3} (line with filled squares). The neutral stability line with filled square for Re_{c3} seems to consist of two distinct curves which intersect with each other at $A \sim 2.1$, which suggests an exchange of the instability modes.

The Strouhal number $St(\equiv L_0 f/3hU_{\max})$, where f is the frequency in the time periodic flow, is evaluated from the numerical data and is depicted in Fig. 8. The Strouhal number also changes stepwise with a continuous change of the aspect ratio A. The jump of St at $A \sim 2.1$ corresponds to that of Re_{c3} in Fig. 7. This also remind us an exchange of instability modes. The instability where St changes stepwise with a continuous change of a parameter is characteristic of impinging free shear layer instability (IFSLI). The instability (IFSLI) occurs when a jet like stream impinges on a object (see

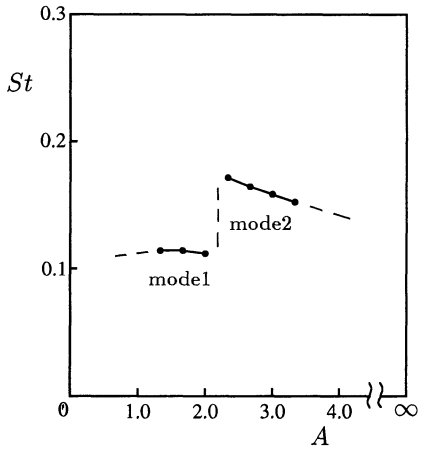

Figure 8. Strouhal number St.

Rockwell and Naudascher, 1979).

Impinging free shear layer instability

The jumps of values of St and Re_{c3} remind us an exchange of the instability modes, which we confirm by showing the flow patterns of the disturbances. The disturbance can be defined by a difference of the time periodic flow from the unstable symmetric flow at the same Reynolds number.

The flow patterns calculated are shown in Fig. 9(a)-9(d). Figure 9(a) shows the time periodic flow at $Re = 1150$ for $A = 4/3$. We have calculated an unstable symmetric solution at the same Reynolds number by assuming the symmetry. The disturbance is calculated by subtracting the symmetric solution from the time periodic solution as depicted in Fig 9(b). The disturbance for $A = 7/3$ calculated in a similar manner is depicted in Fig. 9(d).

The disturbance for $A = 4/3$ has two sets of vortices, whereas the disturbance for $A = 7/3$ consists of three sets of vortices. This difference shows the exchange of the instability modes, so the mechanism of the discontinuous change of St in IFSLI is shown due to the exchange of the instability modes.

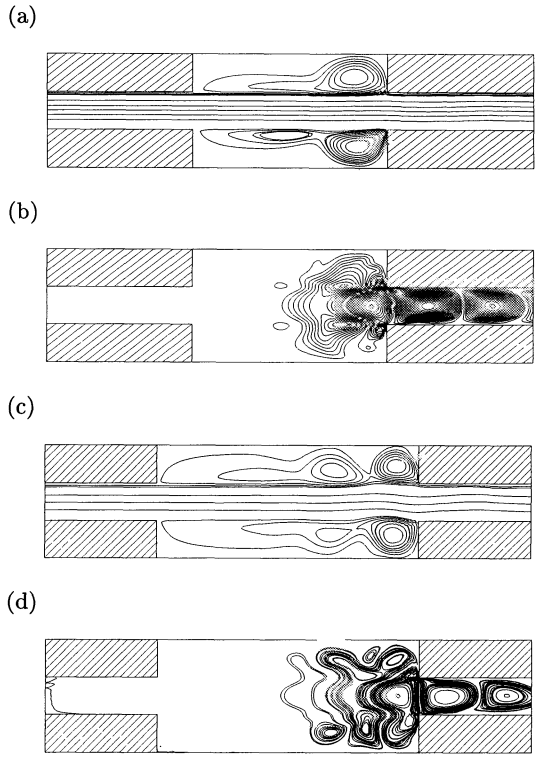

Figure 9. Flow patterns. (a), (b): $A = 4/3$. $Re = 1150$. (c), (d): $A = 7/3$. $Re = 900$. (a), (c); Flow field. (b), (d): Disturbance.

ACKNOWLEDGEMENT

The authors express their cordial thanks to Profs. K. Hirata and H. Yamaguchi for valuable discussion. This work was partially supported by a Grant-in-Aid from the Ministry of Education, Science and Culture and also by Doshisha University's Research Promotion Funds.

REFERENCE

Alleborn, N., Nandakumar, K., Raszillier, H., and Durst, F., 1997, "Further contributions on the two-dimensional flow in a sudden expansion," *J.Fluid Mech.*, Vol. 330, pp. 169-188.

Cherdron, W., Durst, F., and Whitelaw, J. H., 1978, "Asymmetric flow and instabilities in symmetric ducts with sudden expansion," *J.Fluid Mech.*, Vol. 84, pp. 13-31.

Durst, F., Melling, A., and Whitelaw, J. H., 1974, "Low Reynolds number flow over a plane symmetric sudden expansion," *J.Fluid Mech.*, Vol. 64, pp. 111-128.

Fearn, R. M., Mullin, T., and Cliffe, K. A., 1990, "Nonlinear flow phenomena in a symmetric sudden expansion," *J.Fluid Mech.*, Vol. 211, pp. 595-608.

Mizushima, J., Yamaguchi, H., and Okamoto, H., 1996, "Stability of flow in a channel with a suddenly expanded part," *Phys.Fluids*, Vol. 8, pp. 2933-2942.

Rockwell, D., and Naudascher, E., 1979, "Self-sustained oscillations of impinging free shear layers," *Ann. Rev. Fluid Mech.*, Vol. 330, pp. 67-94.